

## Observation of a sample-dependent 37 K anomaly on the lattice parameters of strontium titanate

L. ARZEL<sup>1,2</sup>, B. HEHLEN<sup>1</sup>, F. DÉNOYER<sup>3</sup>, R. CURRAT<sup>2</sup>,  
K.-D. LISS<sup>4(\*)</sup> and E. COURTENS<sup>1</sup>

<sup>1</sup> *Laboratoire des Verres, UMR 5587 CNRS, Université Montpellier II  
F-34095 Montpellier Cedex 5, France*

<sup>2</sup> *Institut Laue-Langevin - BP 156, F-38042 Grenoble Cedex 9, France*

<sup>3</sup> *Laboratoire de Physique des Solides, UMR 8502 CNRS, Université Paris-Sud  
F-91405 Orsay Cedex, France*

<sup>4</sup> *European Synchrotron Radiation Facility  
BP 220, F-38043 Grenoble Cedex, France*

(received 5 August 2002; accepted in final form 16 December 2002)

PACS. 61.50.Ks – Crystallographic aspects of phase transformations; pressure effects.

PACS. 77.84.Dy – Niobates, titanates, tantalates, PZT ceramics, etc.

PACS. 61.10.-i – X-ray diffraction and scattering.

**Abstract.** – The lattice parameters of tetragonal strontium titanate are determined to about 1 part in  $10^6$  with penetrating X-rays. While no peculiarity is detected in a bulk sample, a distinct anomaly at 37 K is observed in an optically polished thin platelet derived from the same single crystal. This suggests that the anomaly is related to a high density of dislocations. A possible mechanism is that dislocations stabilize transverse antiphase boundaries which undergo a ferroelectric transition near 37 K. If so, this transition stresses the boundaries which then strain the bulk leading to the observed anomaly.

The perovskites,  $ABO_3$ , form a large family of compounds with a rich variety of properties finding many applications, in particular dielectric ones. Strontium titanate,  $SrTiO_3$ , is often considered as the paradigm of perovskites. It is cubic at room temperature ( $T$ ) and the ionic radii ideally match the structure, the tolerance factor [1] being equal to 1 to better than 1%. The interest in perovskites does not lie in perfect cubic structures, but rather in the many instabilities that the structure is prone to. Considering crystalline —or ferroic— changes in pure compounds, the instabilities are mainly of two types: i) the ferrodistortive ones that preserve the number  $Z$  of molecular units per primitive cell, and ii) the antiferrodistortive (AFD) ones for which  $Z$  is multiplied by an integer greater than 1.  $SrTiO_3$  exhibits both types of instabilities. It remains cubic with  $Z = 1$  down to  $T_a \cong 105$  K, where it first undergoes an AFD transition with cell doubling [2]. The latter results from alternate rotations of the quite rigid  $TiO_6$  octahedra around one of the three cubic axes, which becomes thereby the tetragonal

---

(\*) Present address: Institut für Werkstofforschung, GKSS-Forschungszentrum - Max-Planck-Strasse, D-21502 Geesthacht, Germany.

axis  $c$ . The corresponding phonon instability is at the  $R$ -corner of the Brillouin zone [3]. The order parameter of the transition is the *staggered* rotation angle  $\phi$ . For rotations around the cubic axis  $\hat{i}$ , it will be written  $\phi_i$ . In addition, a zone center polar mode ( $TO_1$ ) is also very soft [4]. In the absence of the competing AFD deformations, the material would become ferroelectric (FE) around 30 K [5]. Owing to the combined actions of quantum fluctuations *and* AFD competition, the FE transition is suppressed [5] and the dielectric constants stabilize at very high values near liquid-helium  $T$  [6].

In 1991, Müller *et al.* observed by electron paramagnetic resonance (EPR) an additional transition-like anomaly at  $T_q \approx 37$  K [7]. New EPR lines or line broadening did not appear at  $T_q$ , just an anomaly in the crystal-field parameters. The origin of this intriguing observation remained quite debated (see, *e.g.*, [8]). A signature of this effect is absent from many other measurements performed on large samples of good quality [9, 10]. Therefore, the idea arose that the anomaly might be set off by the presence of a high density of structural defects such as those that result from cutting, grinding, or polishing. Indeed, the EPR samples were always small in at least one dimension, often in the shape of thin polished platelets, perpendicular to a  $(110)$  direction and elongated along  $(001)$ . For reasons that are not understood in detail, such platelets spontaneously orient below  $T_a$  with  $c$  in their long direction [11]. In this letter, the lattice constants of a thin polished platelet of  $\text{SrTiO}_3$  are compared to those of a bulk sample of the same origin. An anomaly around 37 K is found in the platelet, as already briefly reported elsewhere [12], while it is absent from the bulk. This suggests that  $T_q$  relates to a high density of dislocations. The available results are consistent with a mechanism implying a FE transition that should occur in transverse antiphase-domain boundaries related to the AFD order, as shown in [13]. However, it must be kept in mind that structural defects can produce many different types of local phase transitions and that these could possibly cause anomalies in this temperature region.

The experiments were performed at the high-energy beam line ID15A of the European Synchrotron Radiation Facility in Grenoble, France [14]. We used the high-resolution triple-axis diffractometer equipped with interferometrically controlled goniometers for the monochromator (M), sample (S), and analyzer (A) axes [15]. The minimum step size on each axis is  $0.1''$  of arc. These angles will be designated by  $\omega_M$ ,  $\omega_S$ , and  $\omega_A$ , respectively. Our first experiment used a thin polished platelet derived from a high-quality colorless Verneuil boule (Earth Chemicals, Kobe, Japan). The platelet size is  $7 \times 2 \times 0.28$  mm, in the directions  $c$ ,  $D$ , and  $D'$ , respectively. The long direction is a cubic axis which becomes the tetragonal  $c$ -axis below  $T_a$  [11], while  $D$  and  $D'$  are face diagonals in the  $(a, b)$ -plane,  $a$  and  $b$  being the other cubic axes. The sample is placed in a He flow cryostat. The X-ray energy is 117 keV, corresponding to a wavelength  $\lambda = 0.106$  Å. A non-dispersive diffraction geometry is employed. The  $7\ 1\ 1$  reflections of highly perfect Si crystals are used for M and A. The sample is in transmission geometry, with  $c$  and  $D'$  in the scattering plane. At this energy the absorption in the thin sample is negligible. Bragg reflections with cubic indices  $0\ 0\ 5$  and  $3\ 3\ 3$  are studied. The corresponding  $d$ -spacings,  $d_{005}$  and  $d_{333}$ , give access to the lattice parameters  $c$  and  $a$  (referred to the primitive cubic cell, as usual). The Bragg angles on M, S, and A will be designated by  $\theta_M$ ,  $\theta_S$ , and  $\theta_A$ , respectively. Upon tracking a Bragg reflection after  $T$  was changed, one first moves  $\omega_S$  to remain on the reflection peak, and then one scans  $\omega_A$  to measure its position. Designating by  $\delta\omega$  and  $\delta\theta$  the angular changes from a reference position, it is easily shown that  $2\delta\theta_S = 3\delta\omega_M - \delta\omega_A$ . Hence, the determination of changes in  $\theta_S$  is independent of the knowledge of  $\omega_S$ , and thus of temperature effects on the angular position of the long stick holding the sample in the cryostat. Even if there is appreciable sample mosaicity, scans in  $\omega_A$  can also be much narrower than those in  $\omega_S$ . With  $\omega_M$  fixed, and for small scattering angles, the Bragg law gives  $\delta d/d \cong (d/\lambda)\delta\omega_A$ . Scans of  $\omega_A$  for the two Bragg reflections studied here have a full

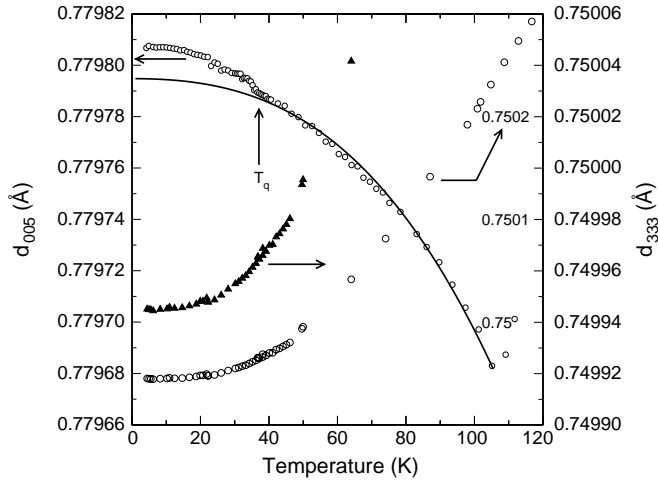


Fig. 1 – Relative  $d$ -spacings measured with penetrating X-rays on a thin polished platelet of SrTiO<sub>3</sub>.  $\Delta d_{005}$  and  $\Delta d_{333}$  are shown on the same vertical scale to emphasize that the anomaly clearly seen on  $\Delta d_{005}$  is at best very weak on  $\Delta d_{333}$ . The full range of  $\Delta d_{333}$  is also shown (large open circles) on a compressed scale (right axis inside). The solid line proportional to  $\phi^2$  is a guide to the eye.

width below  $1''$  of arc. Numerical fitting determines the center of such scans to at least  $0.02''$ . With  $d \sim 0.7 \text{ \AA}$ , one finds that a relative accuracy better than 1 part in  $10^6$  can in principle be achieved on  $\delta d/d$ . In practice, judging from the dispersion in the successive data points upon scanning  $T$ , it appears that such a precision is indeed obtained. These measurements only give the *relative*  $d$ -spacings, *i.e.* the changes  $\Delta d_{005}$  and  $\Delta d_{333}$ . To express the lattice parameters and thus the  $d$ -spacings in absolute terms, we match our results to a literature value of the lattice constant sufficiently above  $T_a$ , *i.e.* outside the region of pretransitional fluctuations,  $a = c = 3.89559 + 2.61192 \times 10^{-5} \times T(\text{K}) \text{ \AA}$  from [16].

Figure 1 shows  $\Delta d_{005}(T)$  and  $\Delta d_{333}(T)$  obtained in two separate runs:  $d_{005}$  is simply proportional to  $c$ ,  $d_{005} = c/5$ , while  $d_{333}$  mostly depends on  $a$ ,  $d_{333} = 1/(3\sqrt{2/a^2 + 1/c^2}) \cong a/5.2$  in the cubic phase. A run consists in cooling the platelet to liquid-He  $T$ , and then raising  $T$  in small steps. After thermalization,  $\omega_S$  is scanned to find the maximum of the selected Bragg reflection, and then  $\omega_A$  is measured across the reflection which amounts to a longitudinal scan of the Bragg peak. The measurement is automated and takes about 15 minutes per step. It should be noted that indeed we found that the platelet spontaneously orients with  $c$  in its longest dimension [11]. Additional Bragg reflections that would arise from ferroic twins were always very weak in  $\omega_S$ -scans compared to the main Bragg peaks. As a guide to the eye, a curve whose  $T$ -dependence is that of  $\phi^2(T)$  determined by EPR [17] is drawn through  $\Delta d_{005}$ . It follows  $\Delta d_{005}(T)$  quite well from  $T_a$  down to  $T_q$ . This curve emphasizes the anomalous increase of  $c$  below  $T_q$ . This observation was reproduced in two separate runs [10]. We only show here the second of these runs, taken with finer  $T$  steps. The anomaly clearly observed on  $c(T)$  is not obvious on  $\Delta d_{333}(T)$ . Using the procedure described at the end of the previous paragraph, the absolute spacings were determined to be  $d_{005} = \Delta d_{005} + 0.77966 \text{ \AA}$  and  $d_{333} = \Delta d_{333} + 0.7499 \text{ \AA}$ . From these two spacings we calculate the tetragonal distortion,  $\varepsilon_t = (c/a - 1)$  shown with triangles in fig. 2b. To obtain  $\varepsilon_t$ , a smooth interpolation was used for  $\Delta d_{333}(T)$ , as the  $T$  steps were not identical for both spacings.

A second experiment was performed on a bulk sample derived from the same Verneuil

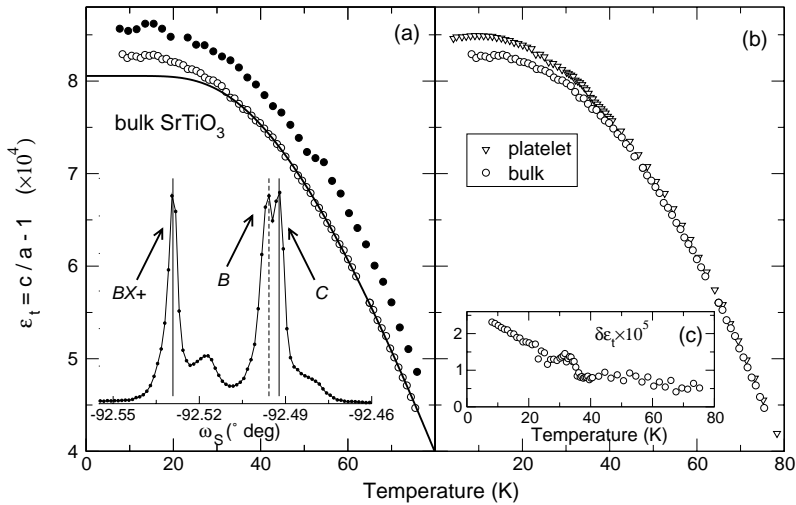


Fig. 2 – (a) Results on the bulk sample: the open dots show the tetragonal distortion  $\varepsilon_t$  on an absolute scale while the full dots are the scattering intensities of the  $13/2\ 11/2\ 1/2$  superlattice reflection in relative units. The solid line is a fit of  $\varepsilon_t$  following the same procedure as in [19]. The inset illustrates an  $\omega_S$ -scan obtained at 10.4 K, with a twin pair indexed  $BX+$  and  $C$ . (b)  $\varepsilon_t$  measured on the platelet (triangles) compared to the bulk sample (open dots). (c) The difference between these two determinations of  $\varepsilon_t$  on an expanded ordinate.

boule. The sample was carefully cut in the shape of a cylinder of 4 mm diameter and 4 mm height. The surface received a fine-grained dull finish. The cylinder axis is along a  $\langle 1\ 1\ 0 \rangle$  crystallographic direction and it is placed vertically in the experiment. The incident energy is now 130 keV, corresponding to  $\lambda = 0.095\ \text{\AA}$ . The sample transmission is approximately 50%, which is acceptable. During this experiment the analyser axis of ID15A was not operational so that a 2-axis configuration was employed. This gives valuable information in such a case because a bulk sample develops orientational domains—or twins—below  $T_a$ . The principle of the measurement is to analyze the splitting of the Bragg reflections that results from twinning and which is proportional to  $\varepsilon_t$  [18]. Hence, the determination is not affected by a change in the origin of  $\omega_S$  with  $T$ , as only differences in  $\omega_S$  at fixed  $T$  values are used. A scan of  $\omega_S$  across the  $0\ 0\ 6$  Bragg reflection—a transverse scan—is illustrated in the inset of fig. 2a. Scans with  $h = k = 0$  lead to particularly simple patterns [19]. In this particular case, the pair of narrow peaks marked  $C$  and  $BX+$  can be indexed as forming a twin [10]. The full width at half-height of the single peaks is below  $20''$ , indicating a very low mosaicity for this Verneuil crystal compared to older ones with mosaicities of  $30''$  or above [20].  $C$  and  $B$  designate grains with the  $c$ -axis exactly along the original  $\langle 0\ 0\ 1 \rangle$  or  $\langle 0\ 1\ 0 \rangle$  cubic directions, respectively, while  $BX+$  is a domain attached to  $C$  with  $c$  approximately in the cubic  $\langle 0\ 1\ 0 \rangle$  direction.  $BX+$  and  $C$  make contact on a  $(0\ 1\ 1)$  plane for strain compatibility so that  $BX+$  is rotated by  $\varepsilon_t$  around the cubic  $\langle 1\ 0\ 0 \rangle$  direction. Scans are performed at increasing values of  $T$  and the five peaks observed are adjusted to Lorentzians. The angular distance between  $C$  and  $BX+$  is then used to extract the  $\varepsilon_t$  values shown in fig. 2a with open dots.

This determination of  $\varepsilon_t$  from the twinning angle is remarkably similar to literature data obtained with 3-axis measurements of the bulk [19]. This is seen by fitting our  $\varepsilon_t$  data above 35 K with the quantum-corrected Landau expression for  $\phi^2$  taken from [21], also used in [19]. This leads to the solid line drawn through the points in fig. 2a, with parameters

$T_c^{qm} = 111.8$  K and  $\eta = 0.60$ , fully compatible with those reported in [19]. Interestingly, this allows to estimate the mean scatter of our data points which is only  $\sim 1.6 \times 10^{-6}$ , nearly as good as found in the 3-axis measurement reported above. The departure of the data from the fitted line below 35 K, quantitatively similar to [19], should not be mistaken as evidence for a “novel phase” as presented there. Indeed there are *many* reasons why this simple theory for  $\phi^2$  might not agree with  $\varepsilon_t$  with such a high precision. Firstly,  $\varepsilon_t$  can easily depart from  $\phi^2$  since the mean thermal expansion in the AFD phase is as large as the strains produced by the transition. Thermal expansion need not be the same along  $a$  and  $c$  and it can contribute to  $c$ - $a$ . Secondly; ref. [21] only takes into account *one* effective soft frequency, while it is an entire soft-phonon sheet which develops a non-trivial shape at low  $T$ . It is well known that it is for this reason that the Barrett formula for the quantum saturation of the dielectric constant [22] is only approximate [23]. Finally, the expression used in [19] stops at the fourth-order Landau coefficient. If the sixth-order term is included, the fit down to 4 K becomes excellent as shown by the first author of [19] in [24]. Thus, we rather believe that the shape of  $\varepsilon_t$  shown in fig. 2a, and in [19] for many other bulk samples, provides no evidence for any anomaly at  $T_q$ . To confirm this view, we also checked on our bulk sample the temperature dependence of the intensity of a superlattice reflection. The integrated intensity of the 13/2 11/2 1/2 reflection is shown by solid dots in fig. 2a. Its structure factor depends only on the oxygen displacements and it is directly proportional to  $\phi^2$ . On heating, the intensity falls somewhat faster than  $\phi^2$  as the Debye-Waller factor gives a very substantial reduction, *e.g.*  $\exp[-2W] \sim 0.6$  near 50 K [10, 25]. The structure factor is also extremely sensitive to the tetragonal orientation —*i.e.* to the order of the Miller indices  $h k l$ — so that a minute rearrangement of domains can easily produce the effects seen near 15 K and 50 K. However, there is no obvious anomaly around 37 K. Hence, except for an unlikely coincidence, neither the Bragg intensity nor the oxygen motions leading to the large Debye-Waller factor are sharply anomalous at  $T_q$ .

Figure 2b shows that our two separate determinations of  $\varepsilon_t$  remarkably agree above  $T_q$ , confirming again the quality of our 2-axis measurement. However, the curves progressively separate below  $T_q$ . To better see this, the  $\varepsilon_t(T)$  of the bulk sample is adjusted to a fourth degree polynomial in  $T$  giving an excellent fit and the result is subtracted from  $\varepsilon_t(T)$  for the platelet. The difference,  $\delta\varepsilon_t$ , is shown in fig. 2c. A small noisy background is observed between  $T_a$  and  $T_q$ . It is difficult at this stage to assert whether this is real or due to systematic errors. The high noise in that region could also relate to the relatively high slope,  $d\varepsilon_t(T)/dT$ . Below  $T_q$  a significant difference develops, with a peak around 30 K, and it then grows almost linearly down to the smallest values of  $T$ . The same general features were observed for the other  $\Delta d_{005}$  measurement. The peak around 30 K showed some differences between the two  $\Delta d_{005}$  runs, being somewhat bigger in the first one.

These observations suggest that a phase-transition-like phenomenon is indeed taking place in the platelet at  $T_q$ , while it does not occur—or not to the same extent—in the bulk. It is natural to invoke an effect in relation with its high optical polish. This polish, obtained with abrasive slurries of progressively finer grain, is required to orient platelets in the tetragonal phase [11]. Thus, the effect most probably pertains to dislocations. A high density of dislocations, approaching  $10^{10}$  cm<sup>-2</sup>, was found near surfaces of SrTiO<sub>3</sub> that had received a *particularly gentle* mechanochemical polish [26, 27]. With our normal polish, dislocations will presumably affect a much deeper region of the material, possibly the entire platelet thickness. Polishing produces slip planes parallel to the surface. It is already known that the Burgers vectors  $\mathbf{b}$  in SrTiO<sub>3</sub> are mostly oriented along  $\langle 110 \rangle$  directions [26]. Hence, for our particular platelet orientation, one expects a substantial concentration of edge dislocations with their cores roughly parallel to  $\mathbf{c}$ , *i.e.* in the slip planes and perpendicular to  $\mathbf{b}$ . Near a core, the region containing the “extra” lattice plane is under high compression, raising the AFD transition

above room  $T$  [26]. The opposite region—the one with the “missing” plane—is under strong extension, which suppresses the AFD transition. The latter region is also the seed for an antiphase boundary (APB) as around the core the phase of  $\phi_3$  changes by  $\pi$  owing to  $\mathbf{b}$ . Hence, such dislocations do stabilize *transverse* APBs which could then extend far into the bulk.

Antiphase-domain boundaries are planar defects in the phase of  $\phi$ . These are too costly in energy to be abundant on a mere statistical basis in structurally perfect samples [13, 28]. They can be of two extreme types, *longitudinal* (or *easy*) that are perpendicular to  $\mathbf{c}$  and *transverse* (or *hard*) that are parallel to  $\mathbf{c}$  [13]. In spite of their high energy, the former have been observed to be extremely frequent—on the near atomic scale—in very thin samples used in transmission electron microscopy [26]. Hard boundaries are a few times more energetic than easy ones. They are quite thick, of the order of 100 Å, and of the Néel type [13]. This means that the vector  $\phi$  is essentially perpendicular to the boundary plane in the middle of the APB. This strongly favors the appearance of ferroelectricity. The reasons can be understood from [5]. Separating the effects of pure octahedra rotations from these of pure AFD strains on the soft FE-mode frequencies  $\omega_a$  and  $\omega_c$ , it was found that in the bulk it is the rotation around  $\mathbf{c}$  that raises considerably the frequency of the soft mode  $\omega_c$  while it decreases  $\omega_a$ , and that elongations along  $\mathbf{c}$  decrease  $\omega_c$  [5]. In the middle of a hard APB, there is indeed an elongation along  $\hat{3}$  which is imposed by the AFD strains in the adjacent domains. The absence of rotation around  $\hat{3}$ , the presence of rotation perpendicular to  $\hat{3}$ , and this strain, all concur to produce a FE transition in the boundary with the polarization  $\mathbf{P}$  along  $\hat{3}$ . The calculations in [13] show that this happens between 35 and 40 K, corresponding remarkably well with the value  $T_q$  found experimentally.

The FE transition in the boundary generates stresses in its plane: an expansion along  $\mathbf{c}$  and a much smaller compression in the perpendicular direction [12, 13]. The equilibration of these stresses by the bulk of the sample produces additional elongations, written  $\delta c$  for  $\mathbf{c}$  and  $\delta a$  for  $\mathbf{a}$ , which grow with  $T_q - T$  in mean-field theory. Designating by  $t$  the mean boundary thickness and by  $L$  their mean separation, one estimates from the size of  $\delta c$  that  $t/L \sim 0.1$  or that about 10% of the sample volume must be occupied by hard APBs [12]. This gives  $L \sim 1000$  Å, which is consistent with the expected dislocation density. The effect on  $d_{333}$ , that we write  $\delta d_{333}$ , is approximately proportional to  $2\delta a + \delta c$  and therefore quite a bit weaker than  $\delta c$  because  $\delta a \sim -\delta c/4$ . We estimate  $\delta d_{333} \sim 0.1\delta d_{005}$  which explains why no effect near  $T_q$  can be recognized on  $\Delta d_{333}$  in fig. 1. The peak observed on  $\delta\varepsilon_t$  around 30 K is not understood in detail. It might be due to a rearrangement of domains owing to forces between walls associated with their polarization. This might explain that it does not necessarily reproduce well from measurement to measurement, as it may depend on sample history, or also on the particular region of the sample explored by the X-ray beam.

The main conclusion of this study is that a lattice anomaly on  $\mathbf{c}$  is observed on a thin polished platelet while it seems absent from a bulk sample derived from the same crystal. This anomaly starts below 37 K, a value remarkably close to the  $T_q$  of [7]. It can be accounted for by a ferroelectric transition taking place inside antiphase-domain boundaries [13] that are stabilized by edge dislocations. Although this might provide the clue for  $T_q$ , it is clear that our specific model remains speculative at this stage. The main issue is whether a sufficient density of hard APBs is effectively present. Other local transitions could be caused by dislocations, even superconducting ones along dislocation cores [29] which might be better in line with the initial proposal [7]. It is however difficult to picture how a superconducting transition in dislocation cores (which are essentially one-dimensional objects) could produce a lattice anomaly of the size observed. On the other hand, former explanations for  $T_q$ —which invoked the quantum phase coherence of an unknown bulk excitation—seem rather unlikely in a situation where the number of low-frequency branches is so very high, as already discussed in [8]. We

hope that our observations will stimulate more detailed experimental investigations of: i) the dislocation distribution produced in polishing thin SrTiO<sub>3</sub> platelets, ii) the mechanism leading to their spontaneous tetragonal orientation, iii) the formation and stabilization of antiphase boundaries, and iv) the ferroelectric transition in hard boundaries.

\* \* \*

One of us (EC) thanks Prof. A. K. TAGANTSEV for enlightening discussions.

## REFERENCES

- [1] MEGAW H. A., *Proc. Phys. Soc. London*, **58** (1946) 133.
- [2] UNOKI H. and SAKUDO T., *J. Phys. Soc. Jpn.*, **23** (1967) 546.
- [3] SHIRANE G. and YAMADA Y., *Phys. Rev.*, **177** (1969) 858.
- [4] COWLEY R. A., *Phys. Rev. Lett.*, **9** (1962) 159.
- [5] YAMANAKA A., KATAOKA M., INABA Y., INOUE K., HEHLEN B. and COURTENS E., *Europhys. Lett.*, **50** (2000) 688.
- [6] MÜLLER K. A. and BURKARD H., *Phys. Rev. B*, **19** (1979) 3593.
- [7] MÜLLER K. A., BERLINGER W. and TOSATTI E., *Z. Phys. B*, **84** (1991) 325.
- [8] COURTENS E., *Ferroelectrics*, **183** (1996) 25.
- [9] HEHLEN B., Doctoral Thesis, University of Montpellier 2 (1995).
- [10] ARZEL L., Doctoral Thesis, University of Montpellier 2 (2001).
- [11] MÜLLER K. A., BERLINGER W., CAPIZZI M. and GRÄNICHER M., *Solid State Commun.*, **8** (1970) 549.
- [12] ARZEL L., HEHLEN B., TAGANTSEV A. K., DÉNOYER F., LISS K.-D., CURRAT R. and COURTENS E., *Ferroelectrics*, **267** (2002) 317.
- [13] TAGANTSEV A. K., COURTENS E. and ARZEL L., *Phys. Rev. B*, **64** (2001) 224107.
- [14] TSCHENTSCHER T. and SUORTTI P., *J. Synchr. Radiat.*, **5** (1998) 286.
- [15] LISS K.-D., ROYER A., TSCHENTSCHER T., SUORTTI P. and WILLIAMS A. P., *J. Synchr. Radiat.*, **5** (1998) 82.
- [16] OHAMA H., SAKASHITA H. and OKAZAKI A., *Phase Transit.*, **4** (1984) 81.
- [17] MÜLLER K. A., BERLINGER W. and WALDNER F., *Phys. Rev. Lett.*, **21** (1968) 814.
- [18] NEUMANN H.-B., POULSEN H. F., RÜTT U., SCHNEIDER J. R. and V. ZIMMERMANN M., *Phase Transit.*, **55** (1995) 17.
- [19] HÜNNEFELD H., RÜTT U., SCHNEIDER J. R. and KAPPHAN S., *J. Phys. Condens. Matter*, **10** (1998) 6453.
- [20] HÜNNEFELD H., NIEMÖLLER T., SCHNEIDER J. R., RÜTT U., RODEWALD S., FLEIG J. and SHIRANE G., *Phys. Rev. B*, **66** (2002) 014113.
- [21] SALJE E. K. H., WRUCK B. and THOMAS H., *Z. Phys. B*, **82** (1991) 399.
- [22] BARRETT J. H., *Phys. Rev.*, **86** (1952) 118.
- [23] VAKS V. B., *Introduction to the Microscopic Theory of Ferroelectrics* (Nauka, Moscow) 1973 (in Russian).
- [24] HÜNNEFELD H., Doctoral Thesis, University of Hamburg (2000).
- [25] JAUCH W. and PALMER A., *Phys. Rev. B*, **60** (1999) 2961.
- [26] WANG R., ZHU Y. and SHAPIRO S. M., *Phys. Rev. Lett.*, **80** (1998) 2370; *Phys. Rev. B*, **61** (2000) 8814.
- [27] HIROTA K., HILL J. P., SHAPIRO S. M., SHIRANE G. and FUJII Y., *Phys. Rev. B*, **52** (1995) 13195.
- [28] CAO WENWU and BARSCH G. R., *Phys. Rev. B*, **41** (1990) 4334.
- [29] GUINEA F., *Europhys. Lett.*, **7** (1988) 549.